Heterogeneous Catalysis

Selective Propene Epoxidation on Immobilized Au$_{6-10}$ Clusters: The Effect of Hydrogen and Water on Activity and Selectivity**

Sungsik Lee, Luis M. Molina,* María J. López, Julio A. Alonso, Bjørk Hammer, Byeongdu Lee, Sönke Seifert, Randall E. Winans, Jeffrey W. Elam, Michael J. Pellin, and Stefan Vajda

Propylene oxide (PO) is an important intermediate bulk chemical that is used in the production of polyurethane and polyols. This product is now commercially produced using either the chlorohydrin or the hydroperoxide routes. Each of these routes has its own limitations,[1] owing to the production of undesired chlorinated byproducts or high cost of the H_2O_2 reactant. A new possibility has arisen based on the experiments performed by M. Haruta et al., wherein small gold nanoparticles were used for the direct propene oxidation by an O_2/H_2 mixture.[2] This new catalyst, if supported on either TiO_2 or titanium silicalite zeolites, converts between 1–10% propene (depending on the support) with a very high selectivity (greater than 90%). Although those results make the use of nanoscale gold very promising, several issues still have to be clarified and improved to employ this catalyst in practical applications. The selectivity of these particles is extremely sensitive to their size and shape, with particles smaller than 1.5–2.0 nm mainly producing propane and particles larger than 4–5 nm assisting oxidation of propene to CO_2 and H_2O. The other limitation in this reaction is the consumption of hydrogen, which should be as low as possible or, if possible, be suppressed altogether for economical reasons. As the stability of the catalysts should be improved for practical applications, there is a need to study the properties and detailed reaction mechanisms of these catalyst systems, and to look for related new catalysts with improved features.

Herein we present the results of an experimental and theoretical study of the catalytic activity of soft-landed subnanometer gold clusters (Au$_6$–Au$_{10}$) for propene epoxidation. Several studies have found a high catalytic activity for similar systems in a number of reactions.[3] Interestingly, for small gold clusters, the activity does not seem to depend very strongly on the type of oxide support.[4] Irreducible oxides are as good as the reducible oxides as supports, as long as the oxide surface contains defects that serve as traps and activate the catalysts.[5] With this in mind, we designed a new type of gold-cluster-based catalyst that is highly active and selective for direct propene epoxidation. The work presented herein comprises the following: 1) amorphous alumina films are used as support instead of the usual titania-based oxides; 2) subnanometer gold clusters are employed instead of larger nanoparticles; and 3) water vapor can replace the expensive and dangerous use of hydrogen in the gas mixture. Ab initio DFT calculations comparing Au/TiO_2 and Au_n/Al_2O_3 support the experimental results, assigning a higher activity to the alumina-supported subnanometer gold clusters owing to easier formation of reaction intermediates. The calculations also confirm that different reaction mechanisms take place for both types of catalysts.

The fabrication of the supported gold model nanocatalysts involves several steps. A thin three-monolayer (3ML) alumina film was initially grown by atomic layer deposition (ALD)[6] on top of naturally oxidized silicon wafers, providing a rough and amorphous support. Such morphology prevents sintering of the subnanometer catalysts under reaction conditions that usually lead to the loss of highly size-dependent activity and selectivity. Earlier studies confirmed the exceptional stability of the platinum clusters on ALD alumina films.[7] A distribution of cationic gold clusters in the range Au_6^+ to Au_{10}^+ (hereafter referred to as Au_n) were then

[*] Dr. L. M. Molina, Prof. M. J. López, Prof. J. A. Alonso
Departamento de Física Teórica, Atómica y Óptica
Universidad de Valladolid, 47011 Valladolid (Spain)
Fax: (+ 34) 983-423-013
E-mail: lmolina@fta.uva.es

Dr. S. Lee, Dr. S. Vajda
Chemical Sciences and Engineering Division, Argonne National
Laboratory, 9700 South Cass Avenue, Argonne, IL 60439 (USA)

Prof. B. Hammer
iNano and Department of Physics and Astronomy
University of Aarhus, Ny Munkegade, 8000 Aarhus C (Denmark)

Dr. B. Lee, Dr. S. Seifert, Dr. R. E. Winans
X-ray Sciences Division, Argonne National Laboratory
9700 South Cass Avenue, Argonne, IL 60439 (USA)

Dr. J. W. Elam
Energy Systems Division, Argonne National Laboratory
9700 South Cass Avenue, Argonne, IL 60439 (USA)

Dr. M. J. Pellin
Materials Sciences Division, Argonne National Laboratory
9700 South Cass Avenue, Argonne, IL 60439 (USA)

Dr. S. Vajda
Center for Nanoscale Materials, Argonne National Laboratory
9700 South Cass Avenue, Argonne, IL 60439 (USA)
and
Department of Chemical Engineering, School of Engineering &
Applied Sciences, Yale University
9 Hillhouse Avenue, New Haven, CT 06520 (USA)

soft-landed on the alumina film, whilst still keeping surface coverage below 0.03ML to prevent the clusters from sintering. Finally, to fully prevent the clusters from sintering, an additional ALD alumina layer (about 2ML thick) was grown selectively to avoid the overcoating of the supported Au_n clusters, leaving them firmly attached at the bottom of a shallow well in the substrate. The reaction experiments were carried out in a reactor by feeding various gas mixtures at 133 kPa (C_3H_6/O_2, $C_3H_6/O_2/H_2$, and $C_3H_6/O_2/H_2O$ in helium), and simultaneous X-ray scattering was used to monitor the size of the gold clusters. No change in cluster size, monitored by grazing-incidence small-angle X-ray scattering (GISAXS), was observed over several hours during the experiments, thus confirming that the immobilized gold clusters were resistant to sintering. Sintering was found, however, in the absence of the extra overlayer of alumina.

Figure 1a,b shows the turnover frequency (TOF) for propene oxide and acrolein coproduct formation at various compositions of the gas mixture, as a function of temperature and of reaction time. In all cases, a large activity is found, although qualitative differences are found in the stability. The propene/O_2 mixture was initially very active at 200°C, but its activity decreases steadily with time. Adding either H_2 or H_2O reverses this trend, and the activity slowly increases with time
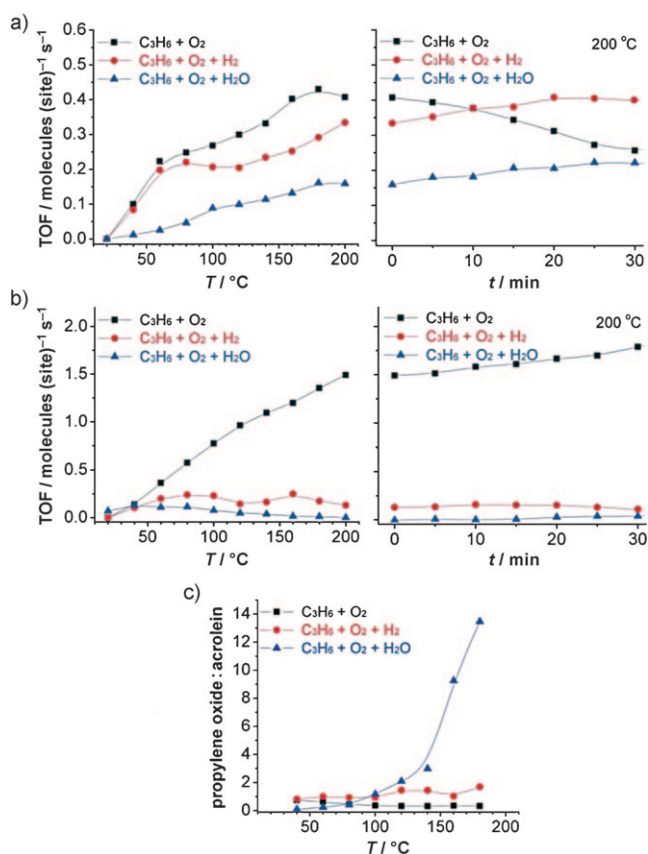

Figure 1. a) Propene oxide formation as a function of temperature (left) and time (right, monitored at 200°C) for various compositions of the gas feed. b) Formation of acrolein as a function of temperature (left) and time (right, monitored at 200°C) for various compositions of the gas feed. c) Temperature-dependent ratio of propylene oxide to acrolein. ■ C_3H_6/O_2, ● $C_3H_6/O_2/H_2$, ▲ $C_3H_6/O_2/H_2O$.

for $C_3H_6/O_2/H_2O$. Thus, we can conclude that under steady-state conditions, the presence of surface hydroxy groups at the perimeter of the cluster is crucial. As the reaction proceeds, the surface hydroxy groups are lost, and in absence of H_2 or H_2O are not replenished at the perimeter of the clusters. Different slopes below or above 100°C are found in all reactivity plots, suggesting slightly different reaction mechanisms with increasing temperature. Based on the above data, the activation energy for the formation of propene oxide are 26–34 kJ mol^{-1} and 6–10 kJ mol^{-1} for the $T < 100$°C and $T > 100$°C regions, respectively. Acrolein production is strikingly different, and for the propene/O_2 feed there is a high activity, which actually increases with time at 200°C. With co-fed H_2, much less acrolein was formed, and already at 100°C the production levels off, indicating that excess oxygen in the surface promotes acrolein, whereas the surface hydroxy groups favor propene oxide formation. The most interesting results are found if water vapor is co-fed, for which formation of acrolein is almost completely suppressed.

Plotting the temperature-dependent ratio of propene oxide versus acrolein (Figure 1c), an estimation of the catalyst selectivity is obtained. Without H_2 or H_2O, we find a 1:2 ratio, whereas selectivity slightly improves with H_2, and we obtain ratios between 1:1 and 2:1 depending on the temperature. The most spectacular results are found for water, for which up to 14:1 ratios are observed at 200°C. This makes propene/O_2/H_2O an optimal mixture for practical applications of this type of catalyst: the slightly smaller activity for propene oxide production is well compensated by the high selectivity. Copper catalysts also produce propene oxide without hydrogen, although with poorer selectivity.[8]

To understand the activity of these new Au_n/Al_2O_3 model catalysts for propene epoxidation and the underlying mechanisms, we performed ab initio DFT simulations of the adsorption of C_3H_6 on a model of the alumina-supported small gold nanoclusters. Such supported gold nanoclusters are formed by taking a large slab of the α-Al_2O_3(0001) surface, excavating a hole in it (keeping the slab at 2:3 stoichiometry), and placing a Au_7 cluster inside, followed by complete relaxation of the structure (Figure 2a). The hole-induced disorder results in significant reconstruction, making the support chemically close to amorphous alumina. In addition, we compare the results obtained with analogous simulations for a model of TiO_2-supported gold nanoparticles, which is the prototypical gold catalyst for propene epoxidation.[2] TiO_2-supported gold nanoparticles are formed by supporting a one-dimensional gold rod on an anatase-TiO_2(101) slab (Figure 2b). This approach was motivated by the results of Nijhuis et al.,[9] which provide evidence for the active interfacial gold-oxide region (also active for CO oxidation)[10] that is responsible for the epoxidation reaction between propene and substrate oxygen.

For a more realistic modeling we added a sizable number of hydroxy groups (up to 14), which are likely to adsorb on the alumina surface in presence of O_2/H_2 or O_2/H_2O. Table 1 shows the energetics for the sequential dissociative adsorption of up to seven water molecules on the Au_7/Al_2O_3 model catalyst. Hydroxy groups are easily formed with binding energies of 1–2 eV for the first four pairs and 0.5–1.0 eV for
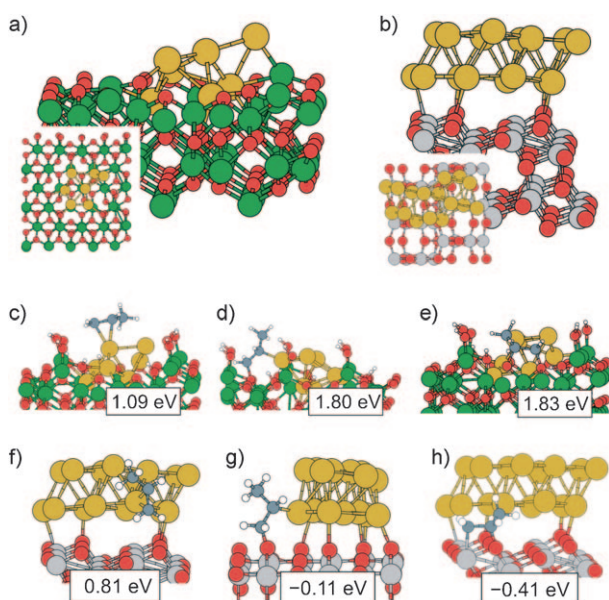
Figure 2. Side and top (smaller inset) views of the relaxed structure for the non-hydroxylated a) Au_7/Al_2O_3 and b) Au/TiO_2 model catalyst. Most relevant relaxed structures and binding energies (with respect to gas-phase propene) for propene adsorption at c–e) Au_7/Al_2O_3 and f–h) Au/TiO_2. Al green, Au yellow, H white, O red, C gray, Ti light gray.

Table 1: Cumulative binding energies (in eV, with respect to water vapor) for dissociative adsorption of up to n water molecules on Au_7/Al_2O_3, where $E_b(n) = nE(H_2O,g) + E(Al_2O_3) - E(nH_2O/Al_2O_3)$.

n	1	2	3	4	5	6	7
$E_b(n)$	2.75	3.57	4.65	6.90	7.56	8.47	8.99

higher coverage, confirming the high reactivity of the surface towards saturation of the dangling bonds.[11] In contrast, the TiO_2 surface is much less reactive; analogous tests provide dissociative binding energies of only 0.5–0.6 eV for the first pair of H_2O molecules. Therefore, a slab with 12 surface hydroxy groups was chosen as the final model for Au_7/Al_2O_3, which corresponds to the situation in which the adsorption of the hydroxy groups begins to saturate (Figure 2 c–e). For Au/ TiO_2, the clean system was chosen, as tests in the presence of a single hydroxy group yielded similar propene/propene oxide binding energies.

The results for propene adsorption on both catalysts (Au_7/Al_2O_3 and Au/TiO_2) are shown in Figure 2 c–e and Figure 2 f–h, respectively. Three possibilities were found: 1) the adsorption of gas-phase propene onto gold by interaction of the intact double C=C bond and a low-coordinate gold atom (Figure 2 c,f). The strong binding (0.81 and 1.09 eV) suggests an easy adsorption, which is in agreement with experiments by Ajo et al. (Au/TiO$_2$) and by Nijhuis et al. (Au/SiO$_2$), showing that propene binds to gold by π bonding.[12] Figure 2 d,g shows the diffusion to the gold/oxide interface, which is probably the second step of the reaction and involves the replacement of the double C=C bond by a single C—C bond to form the two new covalent C—surface bonds. In case

of Au_7/Al_2O_3 (Figure 2 c,d), the change is almost barrierless, with a highly stable final state (1.5–1.8 eV binding, depending on the site around Au_7). This conformer, which bridges an oxygen surface anion and a gold atom, resembles the metallacycle conformers already found as key intermediates for ethene epoxidation on silver catalysts.[13] For the formation of the metallacycle, reactive non-hydroxylated oxygen anions around the gold cluster must exist. Therefore, the removal of the hydroxy group by the interaction with adsorbing O_2 or H_2O becomes essential. The removal of the hydroxy groups is also aided by the decrease in hydroxy group stability at high coverage found above. We also analyzed the interaction between gold-adsorbed propene and coadsorbed hydroxy groups, which could give rise to the C_3H_6OH intermediates, but found that there is instead a strong repulsion. In contrast, Au/TiO_2 is much more inert to the formation of metallacyclic intermediates (Figure 2 g), and although such metallacycles are metastable, they are slightly unstable towards desorption to gas-phase propene.

The third possibility is shown on Figure 2 e, in which propene binds to the substrate through two covalent C—O bonds, resembling the bidentate propoxy species recently found during propene epoxidation at Au/TiO_2 by Nijhuis et al.[9] The stability of the propoxy species is as high as the gold-oxide bridging mode, thus demonstrating that in a small cluster, such as Au_7, the C—Au bonds can be as stable as the C—O bonds with the oxide. As for the Au/TiO_2 system, Figure 2 h shows the most stable metallacycle conformer that forms on the oxide surface, with propene bridging a titanium cation and an oxygen anion (a configuration analogous to the one in Figure 2 e is around 0.5 eV less stable). Again, propene adsorbs in a metastable fashion with endothermic binding, confirming the much more inert character of the Au/TiO_2 system relative to the Au_7/Al_2O_3 system, which traps propene more efficiently by easy formation of metallacycle propene oxide intermediates. At this point, it is interesting to mention that several very recent experiments[14] suggest that the presence of very small Au_n clusters could account for the observed activity in nanoparticle-supported gold catalysts on certain reactions. We have analyzed the stability of the conformer in Figure 2 g at a TiO_2-supported Au_7 cluster and find an only slightly larger binding energy (0.1–0.3 eV, depending on the coverage by the hydroxy groups; see the Supporting Information), which highlights the qualitative difference between alumina and titania supports.

Structures and energetics for the final reaction step, that is, the formation of propene oxide, are shown in Figure 3. Owing to the differences for propene adsorption, different pathways are explored for either Au/TiO_2 or Au_7/Al_2O_3. For Au/TiO_2, direct surface oxygen removal is not feasible and calls for other sources of reactive oxygen; as extensive simulations of the coadsorption and reaction of H_2/O_2 at the Au/TiO_2 catalyst show that ·OOH radicals easily form after reaction of O_2 with surface hydroxy groups (formed after H_2 dissociation at the gold nanoparticle),[15] which can be perceived as oxidizing agents. Figure 3a shows that after a low 0.5 eV energy barrier, the peroxo radical dissociates and a strongly bound (1.59 eV) propene oxide metallacycle is formed, which can be identified as the bidentate propoxy
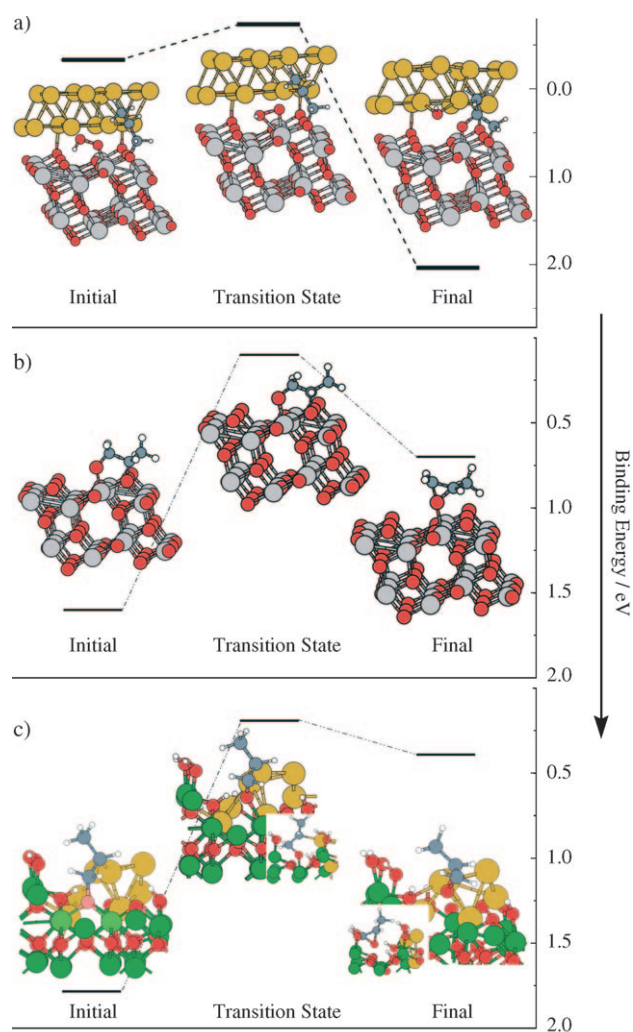
Figure 3. a) Structures and reaction energetics for the formation of propene oxide from coadsorbed propene (Figure 2 g) and peroxo ˙OOH radicals at Au/TiO₂ catalysts. b) Reaction energetics for propene oxide desorption from the anatase $TiO_2(101)$ surface. c) Reaction energetics for propene oxide formation at the Au_7/Al_2O_3 model, involving abstraction of substrate oxygen. Insets with rotated views are included for transition and final states. The color code is the same as in Figure 2.

species.[9] The last reaction step involves desorption of these species; Figure 3 b shows that for TiO_2 (the gold particle is omitted now, as test calculations show that it does not modify the C_3H_6O–TiO_2 interaction), this desorption is the most difficult stage of the reaction, taking a moderately high barrier of 1.5 eV to close the metallacycle. The same holds for Au_7/Al_2O_3 (Figure 3 c), with a 1.6 eV barrier for substrate oxygen abstraction. The process involves a gradual detachment of the oxygen atom by breaking each of the three O–Al surface bonds: one when the metallacycle is formed, the second in the transition state, and the third during the formation of the second C–O bond in C_3H_6O. As the process leaves an oxygen vacancy behind, the catalytic cycle will finally be closed by healing it with oxygen.

Comparing the mechanisms for the two systems, some interesting conclusions can be drawn. For Au/TiO₂, reactive peroxo ˙OOH radicals are needed for the formation of C_3H_6O metallacycle intermediates, whereas for Al_2O_3-supported gold clusters they can form directly after C_3H_6 adsorption. Such differences can be related to the replacement of hydrogen by water in the Al_2O_3-supported catalysts; for Au/TiO_2, we find the dissociation of hydrogen at the gold nanoparticle to be an essential part of the process, both for the formation of the surface hydroxy group and for promoting the adsorption of molecular oxygen with subsequent formation of reactive peroxo radicals. In the case of Au_n/Al_2O_3, oxygen takes care of "healing" the vacancies (providing either reactive oxygen adatoms, adsorbed hydroxys, or desorbing water, depending on the neighboring hydroxy concentration). Finally, in both cases the presence of neighboring hydroxy groups is probably important for the process of detachment of propene oxide metallacycles from the substrate.[9] We expect the calculated energy barriers to be lowered upon inclusion of more coadsorbates, such as water, thus bringing the barriers closer to the measured activation energies (see above). The results shown in Figure 1 a (propene/O₂ atmosphere) can probably be interpreted as arising from a situation in which the hydroxy-terminated surface is transformed into an oxygen-terminated situation, leading to an accumulation of adsorbed metallacycles. These metallacycles are difficult to desorb and block the active catalytic sites.

In summary, the results from the experimental and theoretical study are unexpected and surprising in several ways. First, we demonstrate that our model catalysts based on subnanometer gold clusters are active for the partial oxidation of propene (other similar model catalysts are active for CO oxidation).[5] Our work thus complements existing reports on similar activity of larger gold nanoparticles.[1,2] Second, to our knowledge, this is the first catalyt for the C_3H_6/O_2 system which uses alumina as support, instead of the commonly applied titania that was considered essential for the production of ˙OH/˙OOH radicals, which are believed to be needed for the promotion of the partial oxidation step on gold/titania. The results from the simulations confirm the viability of this system, assigning an even more active character to the Au_n/Al_2O_3 interface than to the Au/TiO_2 one. Third, and more important, for Al_2O_3-supported gold subnanometer clusters the expensive and dangerous hydrogen can be replaced by abundant and safe water vapor, which is also an efficient method to maintain the hydroxy equilibrium at the surface. It will be a challenging task to scale up the production of size-selected clusters by other, more conventional methods, but there are very encouraging experimental efforts demonstrating the feasibility of mass production of supported clusters.[16]

The reactants used are gases at 1% concentration in helium, their ratio is kept 2:1 for C_3H_6/O_2 and 2:1:1 for $C_3H_6/O_2/H_2$ and $C_3H_6/O_2/H_2O$. Products are detected on a mass spectrometer (Pfeiffer). Turnover frequencies (TOF) are calculated using calibrated gas mixtures and the count of deposited clusters. Activation energies are estimated from the temperature dependence of the TOFs. DFT simulations used a plane-waves basis,[18] ultrasoft pseudopotentials[19] (scalar-relativistic for gold to take into account relativistic effects), and the Perdew-Wang-91 GGA functional[20] for exchange-correlation effects. Transition states and energy barriers are evaluated with a constrained minimization technique.[21]

[1] T. A. Nijhuis, M. Makkee, J. A. Mouljin, B. M. Weckhuysen, *Ind. Eng. Chem. Res.* **2006**, *45*, 3447–3459.

[2] T. Hayashi, K. Tanaka, M. Haruta, *J. Catal.* **1998**, *178*, 566–575.

[3] P. Pyykkö, *Angew. Chem.* **2004**, *116*, 4512–4557; *Angew. Chem. Int. Ed.* **2004**, *43*, 4412–4456.

[4] M. M. Schubert, S. Hackenberg, A. C. van Veen, M. Muhler, V. Plzak, R. J. Behm, *J. Catal.* **2001**, *197*, 113–122.

[5] A. Sanchez, S. Abbet, U. Heiz, W. D. Schneider, H. Häkkinen, R. N. Barnett, U. Landman, *J. Phys. Chem. A* **1999**, *103*, 9573–9578; S. Lee, C. Y. Fan, T. P. Wu, S. L. Anderson, *J. Am. Chem. Soc.* **2004**, *126*, 5682–5683; G. Pacchioni, S. Sicolo, C. Di Valentin, M. Chiesa, E. Giamello, *J. Am. Chem. Soc.* **2008**, *130*, 8690–8695.

[6] J. W. Elam, S. M. George, *Chem. Mater.* **2003**, *15*, 1020–1028.

[7] R. E. Winans, S. Vajda, B. Lee, S. J. Riley, S. Seifert, G. Y. Tikhonov, N. A. Tomczyk, *J. Chem. Phys. B* **2004**, *108*, 18105–18107; R. E. Winans, S. Vajda, G. E. Ballentine, J. W. Elam, B. Lee, M. J. Pellin, S. Seifert, G. Y. Tikhonov, N. A. Tomczyk, *Top. Catal.* **2006**, *39*, 145–149.

[8] O. P. H. Vaughan, G. Kyriakou, N. Macleod, M. Tikhov, R. M. Lambert, *J. Catal.* **2005**, *236*, 401–404.

[9] T. A. Nijhuis, T. Visser, B. M. Weckhuysen, *Angew. Chem.* **2005**, *117*, 1139–1142; *Angew. Chem. Int. Ed.* **2005**, *44*, 1115–1118.

[10] L. M. Molina, B. Hammer, *Appl. Catal. A* **2005**, *291*, 21–31.

[11] S. P. Adiga, P. Zapol, L. A. Curtiss, *Phys. Rev. B* **2006**, *74*, 064204; S. P. Adiga, P. Zapol, L. A. Curtiss, *J. Phys. Chem. C* **2007**, *111*, 7422–7429.

[12] H. M. Ajo, V. A. Bondzie, C. T. Campbell, *Catal. Lett.* **2002**, *78*, 359–368; T. A. Nijhuis, E. Sacaliuc, A. M. Beale, A. M. J. van der Eerden, J. C. Schouten, B. M. Weckhuysen, *J. Catal.* **2008**, *258*, 256–264.

[13] M.-L. Bocquet, D. Loffreda, *J. Am. Chem. Soc.* **2005**, *127*, 17207–17215; S. Linic, M. A. Barteau, *J. Am. Chem. Soc.* **2003**, *125*, 4034–4035; D. Torres, N. López, F. Illas, R. M. Lambert, *Angew. Chem.* **2007**, *119*, 2101–2104; *Angew. Chem. Int. Ed.* **2007**, *46*, 2055–2058.

[14] A. A. Herzing, C. J. Kiely, A. F. Carley, P. Landon, G. J. Hutchings, *Science* **2008**, *321*, 1331–1335; M. Turner, V. B. Golovko, O. P. H. Vaughan, P. Abdulkin, A. Berenguer-Murcia, M. S. Tikhov, B. F. G. Johnson, R. M. Lambert, *Nature* **2008**, *454*, 981–983.

[15] L. M. Molina, M. J. López, J. A. Alonso, B. Hammer, unpublished results.

[16] B. C. Gates, *Chem. Rev.* **1995**, *95*, 511–522; A. M. Argo, J. F. Odzak, F. S. Lai, B. C. Gates, *Nature* **2002**, *415*, 623–626.

[17] S. Vajda, R. E. Winans, J. W. Elam, B. Lee, M. J. Pellin, S. Seifert, G. Y. Tikhonov, N. A. Tomczyk, *Top. Catal.* **2006**, *39*, 161–166.

[18] M. C. Payne, M. P. Teter, D. C. Allan, T. A. Arias, J. D. Joannopoulos, *Rev. Mod. Phys.* **1992**, *64*, 1045–1097.

[19] D. Vanderbilt, *Phys. Rev. B* **1990**, *41*, 7892–7895.

[20] J. P. Perdew, J. A. Chevary, S. H. Vosko, K. A. Jackson, M. R. Pederson, D. J. Singh, C. Fiolhais, *Phys. Rev. B* **1992**, *46*, 6671–6687.

[21] A. Alavi, P. Hu. T. Deutsch, P. L. Silvestrelli, J. Hutter, *Phys. Rev. Lett.* **1998**, *80*, 3650–3653.